Positive Regulation of Insulin Signaling by Neuraminidase 1

Larbi Dridi,[1] Volkan Seyrantepe,[1] Anne Fougerat,[1] Xuefang Pan,[1] Éric Bonneil,[2] Pierre Thibault,[2] Allain Moreau,[3,4,5] Grant A. Mitchell,[1] Nikolaus Heveker,[5] Christopher W. Cairo,[6] Tarik Issad,[7,8] Alexander Hinek,[9] and Alexey V. Pshezhetsky[1,5,10]

Neuraminidases (sialidases) catalyze the removal of sialic acid residues from sialylated glycoconjugates. We now report that mammalian neuraminidase 1 (Neu1), in addition to its catabolic function in lysosomes, is transported to the cell surface where it is involved in the regulation of insulin signaling. Insulin binding to its receptor rapidly induces interaction of the receptor with Neu1, which hydrolyzes sialic acid residues in the glycan chains of the receptor and, consequently, induces its activation. Cells from sialidosis patients with a genetic deficiency of Neu1 show impairment of insulin-induced phosphorylation of downstream protein kinase AKT, and treatment of these cells with purified Neu1 restores signaling. Genetically modified mice with ~10% of the normal Neu1 activity exposed to a high-fat diet develop hyperglycemia and insulin resistance twice as fast as their wild-type counterparts. Together, these studies identify Neu1 as a novel component of the signaling pathways of energy metabolism and glucose uptake. ***Diabetes*** **62:2338–2346, 2013**

Insulin signaling is a key event in the regulation of glucose homeostasis; its impairment (insulin resistance) is linked to enormous health problems, including type 2 diabetes (T2DM), obesity, hypertension, and cardiovascular disorders (1–3). The signaling cascade starts from binding of insulin to the cell surface insulin receptor kinase (IRK). The receptor is rapidly activated, autophosphorylated at specific tyrosine residues, and internalized into endosomes. The activated IRK phosphorylates substrates, including IRS-1 to -4, which bind to effector molecules such as phosphatidylinositol 3-kinase (PI3K), resulting in their activation (reviewed in 4). Downstream events involve the activation of protein kinase B (Akt), protein kinase A (PKA), and WNK1 (5), leading ultimately to branching intracellular pathways, inducing glucose uptake and regulating cell metabolism, growth, and differentiation. In endosomes, IRK is dephosphorylated and either sent to lysosomes for degradation or recycled to the plasma membrane for another round of binding, activation, and internalization (6). In obesity-related insulin resistance, increased storage of lipids in nonadipose tissues activates protein kinase C (PKC), which phosphorylates IRS-1 at Ser residues, preventing its phosphorylation at Tyr residues by IRK and further activation of PI3K (7–10).

At the same time, a pool of inactive, nonphosphorylated IRK, present in the cell membrane and in endosomes, can be substantial, especially in vitro at saturating insulin concentrations (11). The differences between the insulin-responsive and unresponsive IRK were attributed to both variations in sequence (12) and posttranslational modification, primarily glycosylation (13). Human IRK contains multiple species of complex N-linked glycans (14,15). N-linked glycans are not only important for proper folding, maturation, and targeting of the receptor but also affect its function. For example, a proreceptor bearing excessive glycosylation does not oligomerize or undergo insulin-sensitive autophosphorylation (13), whereas receptors with mutated glycosylation sites lacking glycan chains at Asn624, -730, -743, and -881 showed normal processing and ligand binding but exhibited a constitutively active tyrosine kinase (14). In a similar fashion, the mutated IRK lacking glycosylation at Asn1234 exhibited a threefold increase of basal autophosphorylation (16). Together, the above data show that N-linked glycans play a critical role in the molecular events responsible for IRK activation and signal transduction.

In the current study, we identify sialic acid residues in the N-linked glycan chains of IRK as key factors affecting IRK activity and insulin signaling. We show that the binding of insulin to the receptor rapidly induces its interaction with neuraminidase 1 (Neu1), an abundant lysosomal/plasma membrane enzyme involved in the catabolism of sialylated glycoconjugates and "trimming" of cell surface sialoproteins (17). Neu1 desialylates and activates the receptor, thus providing a feedback mechanism for the regulation of glucose uptake.

RESULTS

Mice deficient in Neu1 rapidly develop glucose intolerance and insulin resistance after being challenged with a high-fat diet. We previously showed that Neu1 potentiates the proliferative response to insulin in cultured skeletal myoblasts (18). To understand whether

From the [1]Division of Medical Genetics, Sainte-Justine University Hospital Research Center, University of Montréal, Montréal, Québec, Canada; the [2]Institute of Research in Immunology and Cancer, University of Montréal, Montréal, Québec, Canada; the [3]Department of Stomatology, Faculty of Dentistry, University of Montréal, Montréal, Québec, Canada; the [4]Viscogliosi Laboratory in Molecular Genetics of Musculoskeletal Diseases, Sainte-Justine University Hospital Research Center, University of Montréal, Montréal, Québec, Canada; the [5]Department of Biochemistry, University of Montréal, Montréal, Québec, Canada; the [6]Alberta Glycomics Centre, Department of Chemistry, University of Alberta, Edmonton, Alberta, Canada; the [7]Institut Cochin, Université Paris Descartes, CNRS (UMR8104), Paris, France; [8]INSERM, U1016, Paris, France; the [9]Physiology and Experimental Medicine Program, The Hospital for Sick Children, University of Toronto, Toronto, Ontario, Canada; and the [10]Department of Anatomy and Cell Biology, Faculty of Medicine, McGill University, Montréal, Québec, Canada.
Corresponding author: Alexey V. Pshezhetsky, alexei.pchejetski@umontreal.ca.
Received 24 December 2012 and accepted 19 March 2013.
DOI: 10.2337/db12-1825
This article contains Supplementary Data online at http://diabetes.diabetesjournals.org/lookup/suppl/doi:10.2337/db12-1825/-/DC1.
V.S. is currently affiliated with the Department of Molecular Biology and Genetics, Faculty of Science, Izmir Institute of Technology, Gulbahce Koyu, Urla, Izmir, Turkey.

Neu1 also regulates the metabolic action of insulin, we studied glucose uptake in the strain of gene-targeted CathAS190A-Neo mice, which have 10–15% of normal Neu1 activity in their tissues (19,20) (see also Supplementary Fig. 1*A*).

Four-month-old male CathAS190A-Neo mice and their WT siblings received either a normal diet (ND) or a diet with an elevated fat content (high-fat diet [HFD]) known to cause obesity, insulin resistance, and diabetes (21). After 2 weeks on HFD, both Neu1-deficient and WT mice had significantly higher body mass as compared with the groups fed with ND (Fig. 1*A*). No significant difference in weight gain was observed between CathAS190A-Neo and WT mice fed with either HFD or ND. Both groups also had similar fat and lean body masses measured by dual energy X-ray absorptiometry (Supplementary Fig. 1*B*). Food consumption was similar in Neu1-deficient and WT mice (Supplementary Fig. 1*C*), suggesting that their energy expenditures were also similar.

Intraperitoneal glucose tolerance tests (IGTTs) conducted after 0, 4, and 8 weeks revealed that HFD-fed Neu1-deficient mice develop glucose intolerance more rapidly than WT controls. Prior to the HFD, mice showed only slight (up to 10–12 mmol/L) increases of blood glucose (Fig. 1*B*), but after 4 weeks on HFD, Neu1-deficient mice were clearly hyperglycemic (Fig. 1*C*). After 8 weeks on HFD, both WT and Neu1-deficient mice showed hyperglycemia but blood glucose levels in Neu1-deficient mice remained significantly higher than in WT mice (Fig. 1*D*).

There was no difference between the groups in the circulating blood insulin level after overnight fasting or in the insulin level measured 30 min after intraperitoneal glucose injections (Fig. 1*E* and *F*), suggesting that Neu1 activity level affects insulin signaling rather than production. This was tested with an insulin tolerance test (ITT) in which fasted mice received intraperitoneal injections of insulin. We found (Fig. 1*G*) that after 1 month on HFD, Neu1-deficient mice showed significantly lower blood glucose response to insulin as compared with the WT group or to Neu1-deficient mice on ND. After 2 months on HFD (Fig. 1*G*), insulin sensitivity in the WT group was also reduced but it was still significantly higher than in the Neu1-deficient mice, which showed almost no response to insulin.

Together, these studies indicate that compared with WT mice, HFD feeding in Neu1-deficient CathAS190A-Neo mice had produced earlier and more severe glucose intolerance due to decreased insulin sensitivity.

Insulin signaling is partially impaired in tissues of Neu1-deficient mice and cells of sialidosis patients. Insulin signaling in the major insulin target tissues, liver and muscle, was studied in Neu1-deficient and WT mice before and after 4 and 8 weeks on HFD. Mice fasted overnight were killed 10 and 20 min after receiving intraperitoneal injections of insulin (1 unit/kg BW), and phosphorylation of IRK, IRS-1, and Akt in the insulin target tissues was studied by Western blots.

Our data indicate that intraperitoneal injections of insulin induce phosphorylation of IRK Tyr1162/1163 residues, previously linked to activation of the receptor (22) (Fig. 2*A*). Similar levels were detected in WT and Neu1-deficient mice receiving ND, but after 1 month on HFD, IRK phosphorylation in liver of Neu1-deficient mice was significantly reduced, suggesting that the dose of insulin was insufficient for activation of the pathway (Fig. 2*A*). In contrast, in the tissues of WT mice, the IRK was still efficiently Tyr phosphorylated. By the end of the second month on HFD, the tissues from both WT and Neu1-deficient mice showed similarly reduced insulin-dependent IRK phosphorylation (data not shown). Similarly, the phosphorylation of AKT was also markedly reduced in Neu1-deficient mice after 1 month on HFD (Fig. 2*B*). A drastic reduction in insulin-dependent AKT phosphorylation was also observed in the muscle tissues of Neu1-deficient mice exposed to HFD (Fig. 2*C*), showing that the effect was not restricted to liver tissue. We also observed similar levels of pSer307-IRS-1 immunoreactivity in liver (Fig. 2*D*) and muscle (not shown) of both control and Neu1-deficient mice, demonstrating that insulin resistance in Neu1-deficient mice is not caused by the excessive serine phosphorylation of IRS-1 by PKC.

To test whether impaired insulin signaling is linked to Neu1 deficiency, we measured insulin-induced AKT phosphorylation in cultured human skin fibroblasts from normal controls and from a patient affected with sialidosis, caused by *NEU1* gene mutations that result in complete deficiency of the enzyme (23). Both cell lines were cultured using insulin-free serum, exposed overnight to serum-free medium to reduce background AKT phosphorylation, and then exposed for 10 min to insulin (20 nmol/L). Western blotting with antibodies against phosphorylated and total AKT showed that insulin induced AKT phosphorylation in normal, but not in sialidosis, fibroblasts (Fig. 2*E*). We further tested if insulin signaling in Neu1-deficient cells could be restored by the treatment of cells with exogenous Neu1 from mouse kidney. The cells were treated for 90 min by medium supplemented with Neu1, which in our previous study was shown to reduce the overall sialylation of the cell surface to the level of control cells (20). Treated and nontreated cells were exposed to insulin, as above. Treatment with exogenous Neu1 restored AKT phosphorylation to the level of normal control cells (Fig. 2*E*).

Desialylation of IRK by Neu1 is linked to its activation. To study the sialylation of the glycan chains attached to the β-chain of human IRK, it was expressed in HEK cells alone or coexpressed with the components of the Neu1 complex, Neu1 and cathepsin A/protective protein (CathA). To facilitate purification, IRK was tagged at the COOH terminus with a CBP to allow purification of the recombinant protein using calmodulin resin and detection with anti-CBP antibodies (24) (Supplementary Fig. 2*A*). Liquid chromatography tandem mass spectrometry (MS) analysis confirmed the identity of the purified IRK β-chain (Supplementary Fig. 2*B*) and identified IRK peptide 1183DIYETDYYR1191 containing phosphorylated Tyr1185 and Tyr1190 residues involved in autocatalytic activation of the receptor (25,26) (Supplementary Fig. 2*C* and *D*), thus indicating that the recombinant IRK retained its native conformation and activity.

To test whether desialylation of IRK depends on the presence of both Neu1 and the ligand, the receptor was expressed alone in HEK cells or coexpressed with Neu1/CathA and the cells were metabolically labeled with ManNAz, an analog of the sialic acid precursor *N*-acetylmannosamine, resulting in biosynthetic labeling of sialic acid–containing glycoconjugates with an azide group (27). ManNAz-labeled cells were induced by insulin (10 min, 20 nmol/L) both with and without pretreatment with the Neu1 inhibitor 2, 3-dehydro-2-deoxy-*N*-acetylneuraminic acid (DANA). IRK was affinity purified, and azido–sialic acid residues in the glycans at its β-chain were modified with biotin-phosphane, which selectively reacts with the azide group. The amount of sialic acid in the IRK β-chain was visualized by blotting

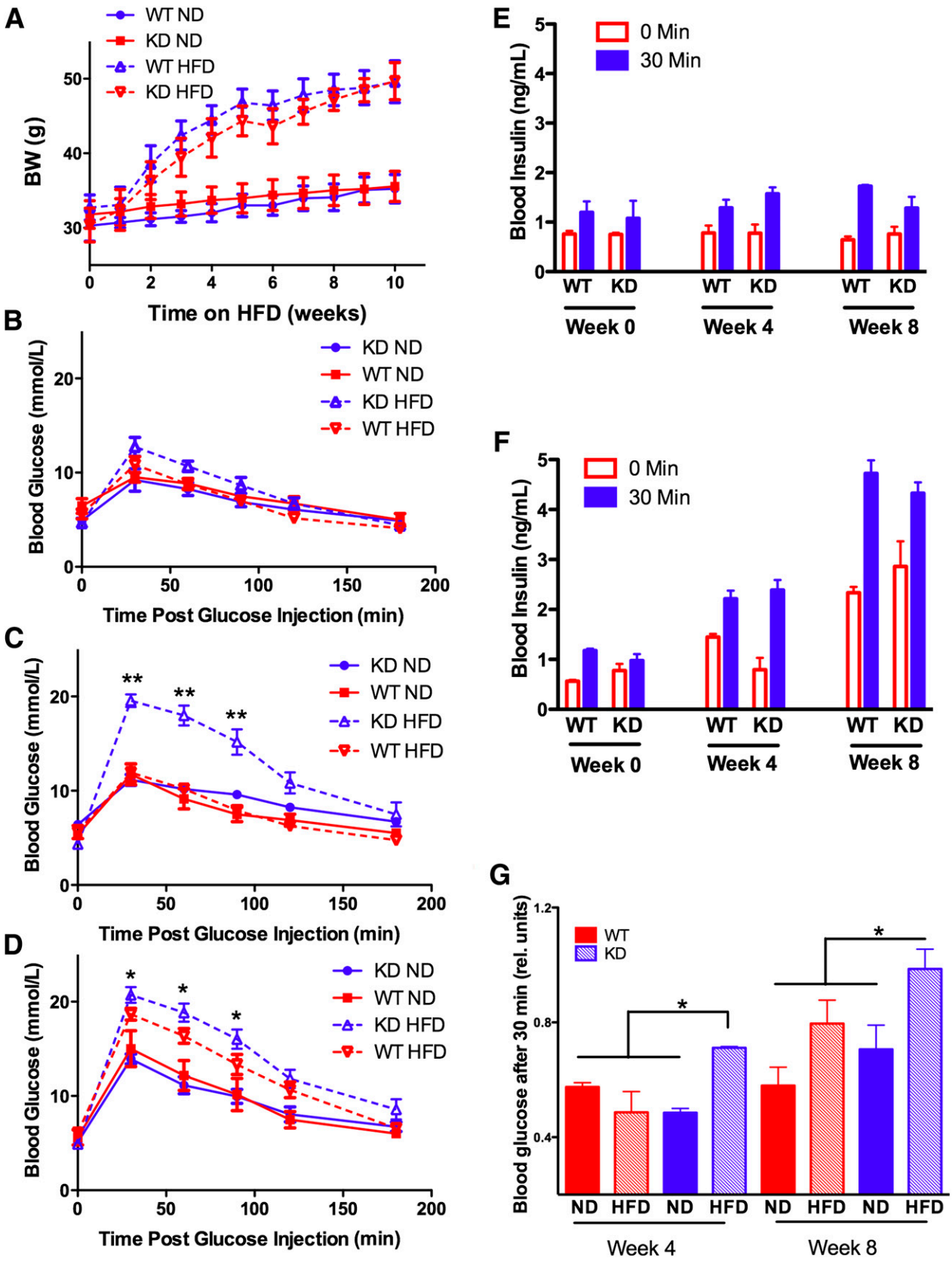

FIG. 1. Diet-induced obesity (*A*), glucose intolerance (*B–D*), and insulin resistance (*E–G*) in Neu1-deficient (KD) mice and their WT siblings. Four-month-old mice were fed for 8 weeks with an HFD or ND. Mice were weighed weekly (*A*). Glucose tolerance tests were performed at week 1 (*B*), 4 (*C*), and 8 (*D*). Fasted (16 h) mice received 1.5 g/kg BW of glucose intraperitoneally, and blood glucose levels were measured before and 30, 60, 90, and 120 min after glucose injection. Insulin levels were measured before and 30 min after glucose injection in mice on ND (*E*) and HFD (*F*). Insulin tolerance tests (*G*) were performed at weeks 4 and 8. Fasted (4 h) mice received intraperitoneal injections of insulin at 1 unit/kg BW, and blood glucose levels were measured before and 90 min after injection. Significant (*$P < 0.05$) or highly significant ($P < 0.001$) difference was detected between WT and KD mouse strains starting from week 4 on HFD. Data were analyzed using general linear model (repeated measurements ANOVA). At least six mice were studied for each genotype. Graphs illustrate one of three independent studies all yielding similar results.**

and staining with HRP-conjugated streptavidin. We found a reduction of staining of the IRK band in Neu1-overexpressing cells and in insulin-treated cells, showing that desialylation is triggered by the ligand and accompanies activation of the receptor. DANA significantly reduced desialylation of the IRK, confirming that Neu1 indeed removes sialic acid residues from the glycan chains of the β-subunit of the receptor (Fig. 3*A*).

The results of the ManNAz labeling experiments correlated with those of lectin blotting where sialylation of the β-chains of affinity-purified IRK was estimated by staining with biotinylated *Maackia amurensis* lectin II (MAL-II). After stripping the blots, autophosphorylation of IRK was measured with monoclonal antibodies against pTyr IRK phosphorylated at Tyr1162/1163, and to determine total amount of receptor, blots were stained with anti-IRK antibodies. Quantitative comparison of blots showed reduced staining of IRK band with MAL-II and increased staining with anti-pTyr1162/1163 in cells overexpressing Neu1, consistent with the hypotheses that Neu1 desialylates IRK and that activation of IRK correlates with desialylation (Fig. 3*B*). An even greater difference in intensity of MAL-II staining was detected for the 180-kDa chain of the IRK precursor, suggesting that in these experimental conditions, Neu1 is also involved in desialylation of the receptor prior to its proteolytic processing (Fig. 3*B*).

To study if desialylation of the receptor is functionally important for autophosphorylation, we studied insulin signaling after blocking the Neu1 access to sialylated glycans at the cell surface proteins by MAL-II lectin treatment. HEK cells overexpressing IRK were pretreated with increasing concentrations (1–100 μg/mL) of MAL-II lectin, treated with insulin as above, and processed to study IRK and AKT phosphorylation by Western blot. Our results (Fig. 3*C*) show that MAL-II blocks insulin-induced activation of IRK and AKT in a dose-dependent manner, suggesting that desialylation of IRK is functionally important for its activation. MAL-II binding to the receptor did not prevent insulin binding, as measured with biotinylated peptide (data not shown).

Insulin binding to IRK induces its interaction with cell surface pool of Neu1. The molecular interactions between Neu1 and IRK in the presence and in the absence of insulin were studied using bioluminescence resonance energy transfer (BRET) (28,29), which can detect transient protein interactions in real time in cells expressing physiological levels of the proteins of interest.

Human IRK and Neu1 fused at COOH termini with yellow fluorescence protein (YFP) and luciferase (hRluc), respectively, were coexpressed with a CathA plasmid in HEK293T cells. In a separate experiment, we demonstrated that the tagged Neu1 is enzymatically active and associates with CathA (Supplementary Fig. 3*A*). The biological activity of hRluc-tagged IRK was demonstrated previously (30). Confocal immunomicroscopy showed that tagged IRK and Neu1 colocalized at the cell surface (Fig. 4*A*), indicating that the tag did not interfere with the plasma membrane targeting of both proteins.

For the BRET assay, HEK cells were treated with the luciferase substrate coelenterazine H in the absence or in the presence of increasing amounts of insulin. In the absence of insulin, we observed only background levels of energy transfer between Neu1-YFP and IRK-RLuc, similar to that observed between IRK-RLuc and YFP used as a negative control. In contrast, incubation of cells with insulin at 5–50 nmol/L resulted in the appearance of a BRET signal (Fig. 4*B*). The signal intensity was significantly different from the background level, and close to that for our positive control (IRK-RLuc/Shc-YFP [31]) (Supplementary Fig. 3*B*), suggesting that IRK forms a complex with Neu1. The BRET signal results from the interaction of Neu1-YFP and IRK-RLuc proteins on the cell surface and not in lysosomes, since hRLuc has a neutral pH optimum and should have reduced enzymatic activity in an acidic lysosomal environment (32). Continuous recordings of BRET signal from cells preincubated with coelenterazine H after rapid injection of insulin into the culture medium showed that the interaction between IRK and Neu1 was induced within 5–10 s after the addition of insulin and was present for at least 30 min, which is consistent with the known kinetics of insulin binding to IRK and activation of the receptor (33).

The interaction between Neu1 and IRK observed by the BRET method was confirmed by coimmunoprecipitation of both proteins with antibodies against IRK. To detect transient interactions between recombinant Neu1 and IRK, HEK cells coexpressing both proteins were treated with the cleavable cross-linking reagent dithiobis (succinimidyl propionate). When proteins precipitated by antibodies against IRK were analyzed by Western blot with antibodies against Neu1, we found a cross-reacting protein band at 49 kDa (Fig. 4*C*), also detected in the total cell lysate and detergent extract, and absent in resin washes or in the lysate of cells not transfected with Neu1 (not shown). The band was present in both insulin-treated and nontreated cells, but its intensity was somewhat higher in the insulin-treated samples.

DISCUSSION

Neu1, the most abundantly expressed mammalian sialidase (34,35), has a well-characterized catabolic function in the lysosome, where it removes the terminal sialic acid residues of oligosaccharides and glycoproteins (reviewed in 36,37). Genetic deficiency of Neu1 causes sialidosis (OMIM #256550) and galactosialidosis (OMIM #256540) (reviewed in 38,39), severe lysosomal storage diseases that manifest with skeletal abnormalities and neurological degeneration. Studies of energy homeostasis, including glucose tolerance, have not been reported in sialidosis and galactosialidosis patients.

Emerging data demonstrate that in addition to its catabolic role in lysosomes, Neu1 can also be targeted to the cell surface (40), where it plays a previously unrecognized role as a structural and functional modulator of cellular receptors, including those for inflammation (TLR4), phagocytosis (FCR-γ), exocytosis (LAMP-1), proliferation (PDGF, EGFR, and TRK), and cell adhesion (integrin β4) (reviewed in 17,41). We have previously shown that Neu1 acts on IRK and the insulin-like growth factor 1 receptor in rat skeletal myoblasts (L6WT), altering their proliferative response to insulin (18,42).

In the current study, in order to understand if the Neu1 action on IRK is physiologically important in vivo, we compared insulin and glucose signaling pathways in WT mice and genetically targeted CathAS190A-Neo mice, which have an ~90% reduction of Neu1 activity. The residual 10% of Neu1 activity suffices to maintain a normal level of lysosomal catabolism of sialoglycoconjugates, and CathAS190A-Neo mice are vital, fertile, and have a normal life span. If they are fed standard mouse chow, Neu1-deficient mice have normal glucose homeostasis and insulin

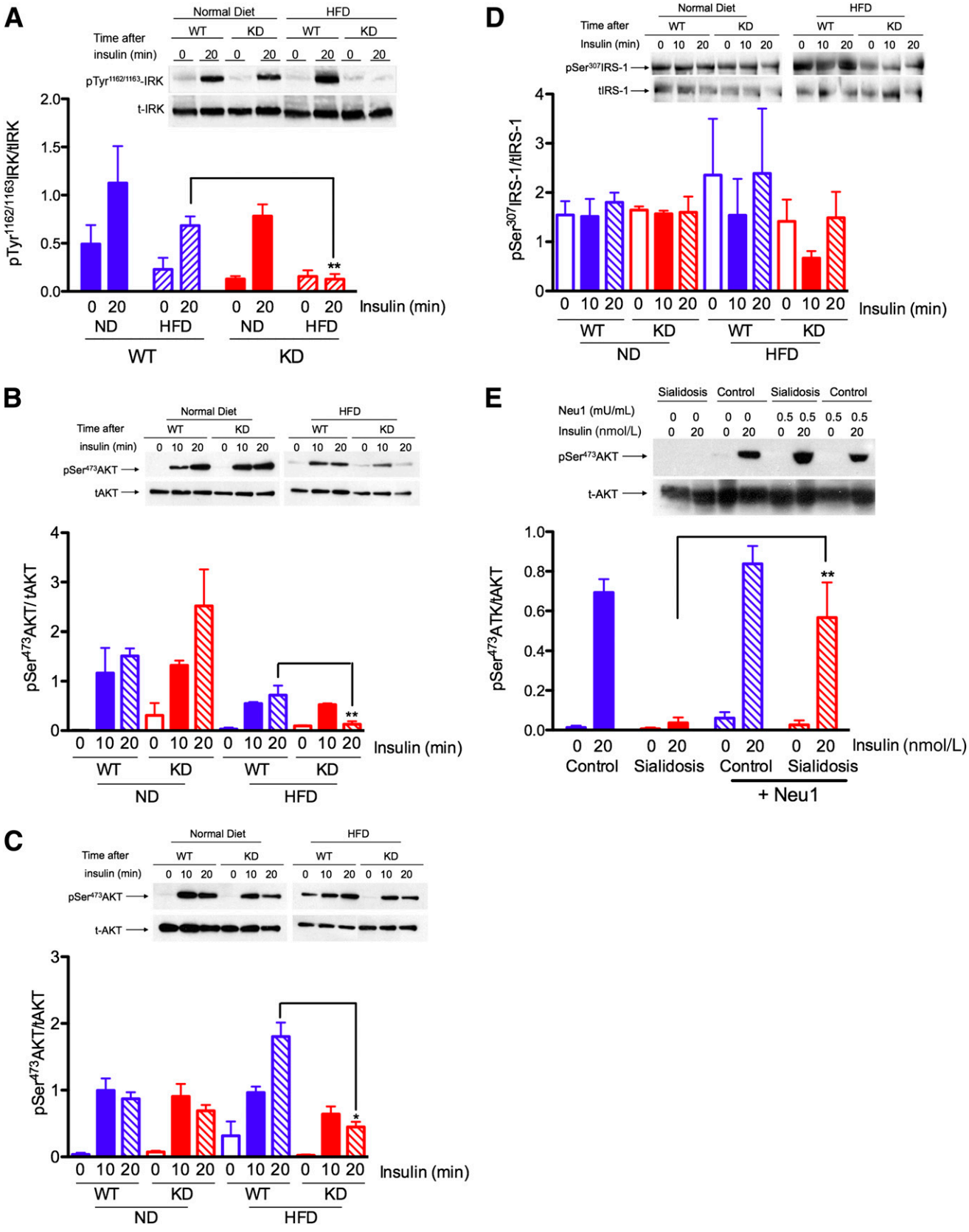

FIG. 2. Impaired insulin signaling in liver (*A*, *B*, and *D*) and muscle (*C*) tissues from Neu1-deficient mice and cells from sialidosis patient (*E*). *A*: Reduced Tyr phosphorylation of β-subunit of IRK. WT and Neu1-deficient (KD) mice fed with ND or HFD for 4 weeks were fasted overnight and killed 20 min after intraperitoneal injections of insulin at 1 unit/kg BW. Saline-injected animals were used as a 0-min time point. Liver homogenates were analyzed by Western blots using antibodies against anti-IRK β-chain and anti-pTyr1162/1163-IRK. Panels show typical results of one of three experiments. Graphs below the panels show quantification of signal intensities using ImageQuant software. Bars show mean values and SD of three independent experiments. *B* and *C*: Reduced Tyr phosphorylation of AKT in liver and muscle tissues. Total liver (*B*) and muscle (*C*) homogenates obtained as described above were analyzed by Western blotting using antibodies against total AKT or AKT phosphorylated at Ser473 residue. Significant (P* < 0.05) or highly significant (***P* < 0.001) difference was detected between WT and KD mouse strains.**

sensitivity; however, they develop glucose intolerance after only a 4-week exposure to an HFD. Mice produced normal levels of insulin, suggesting that hyperglycemia in Neu1-deficient mice results from reduced insulin sensitivity in target tissues. Indeed the levels of insulin-induced phosphorylation of activated IRK and AKT in livers and muscles of Neu1-deficient mice were significantly reduced as compared with that of WT animals. In cultured cells from sialidosis patients, phosphorylation of AKT in response to insulin was also impaired but could be restored by treatment with purified Neu1 sialidase, thus establishing a link between IRK activation and Neu1 activity. Moreover, an inverse correlation was found between the phosphorylation and sialylation levels of IRK expressed in HEK cells. Desialylation of IRK by Neu1 appears to be triggered by direct interaction between the IRK and the Neu1 complex on the cell surface and was clearly induced by insulin, as observed by both BRET and coimmunoprecipitation experiments.

We conclude, therefore, that insulin binding to IRK rapidly induces its desialylation by Neu1, which consequently stimulates its activation. Although the exact molecular mechanisms by which IRK is activated by Neu1 should be defined, we speculate that the presence of sialic acid residues in the glycan chains may affect the conformation and membrane topology of the receptor as well as its ability to interact with other proteins. Of note, the residual level of Neu1 activity in CathAS190A-Neo mice is not changed by HFD (Supplementary Fig. 1*A*). The insulin signaling failure in these mice can, therefore, simply result from the combined effects of reduced IRK activation due to partial Neu1 deficiency and of serine phosphorylation of IRS-1 (7–10). Conversely, we cannot exclude additional "cooperative" interactions between HFD and Neu1 deficiency. For instance, changes in the fluidity or rigidity of cellular membranes induced by HFD (43,44) could affect the conformational changes of the β-chain required for autophosphorylation and/or the molecular interaction of Neu1 and IRK both residing in the lipid rafts at the plasma membrane (45). In future experiments, we plan to test these hypotheses.

It is unclear at present if alterations of Neu1 activity and IRK sialylation can contribute to the insulin resistance and T2DM; however, it is important to emphasize that recent genome-wide association studies in T2DM, including those from our team (46), explain only a modest proportion of known population variance (47). There is a growing suspicion that this missing heritability may be explained by rare and ultrarare variants causing effects strong enough to influence predisposition to common diseases (such as late-onset T2DM) but not strong enough to cause a Mendelian disease (47). It is tempting to speculate that low tissue levels of Neu1 activity influenced by multiple genes, including those coding for CathA, ER chaperons, Golgi enzymes, and transcription factors that generally determine expression levels of lysosomal enzymes and proteins (48), may be among such factors contributing to T2DM in human population.

In conclusion, our data demonstrate the existence of a novel positive feedback mechanism by which a cellular sialidase, Neu1, activates a pool of sialylated inactive IRK on the cell surface in response to the presence of high concentrations of insulin. They also identify sialylation as an important new parameter regulating the signaling pathways for energy metabolism and glucose uptake.

RESEARCH DESIGN AND METHODS

Animals. Previously described (19,20) C57BL/6J mice carrying the c.571AGC>GCA (S190A) point mutation and PGK-Neo cassette in intron 7 of the *CathA* gene, which results in a 90% reduction of Neu1 activity (CathAS190A-Neo), as well as CathAS190A and C57BL/6J wild-type (WT) mice, each of which have normal Neu1 levels, were maintained on a 12-h dark/light cycle with unlimited access to water. Four-month-old (~25 g body weight [BW]) male mice received ad libitum either normal (5% fat and 57% carbohydrate) or high-fat (35% fat and 36% carbohydrate) chow (Bio-Serv). BW and total food consumption were measured. At 0, 4, and 8 weeks, the body composition was measured by dual-energy X-ray absorptiometry scanning (Lunar PIXImus).

IGTT and ITT. IGTT was conducted by intraperitoneal injection of glucose, 1.5 mg/g BW in mice after an overnight fast. Blood from the tail vein was analyzed for glucose levels using an automatic glucometer (Bayer) at 0, 30, 60, 90, 120, and 180 min. Blood samples (50 μL) were collected at 0 and 30 min. After centrifugation at 4,500*g* for 20 min, plasma was collected and stored at −80°C prior to analysis for insulin level using Mouse Insulin ELISA Jumbo kit (Alpco Diagnostics).

ITT was conducted by intraperitoneal injection of insulin (HumulinR; Eli Lilly) at 1 unit/kg BW in mice after a 5-h fast. Blood glucose was measured in tail vein blood at 0–120 min as described above.

Analysis of insulin signaling in animal tissues by Western blot. Mice fasted overnight received intraperitoneal injections of insulin (1 unit/kg BW) and were killed 10 and 20 min later by cervical dislocation. Saline-injected animals were used as a 0-min time point. Tissues were immediately removed and homogenized in RIPA buffer (50 mmol/L HEPES, pH 7.4, 0.1 mmol/L EDTA, 150 mmol/L sodium chloride, 2 mmol/L phenylmethylsulfonyl fluoride, 1% NP40, 2.5% sodium deoxycholate, protease and phosphatase inhibitors; Roche) using tissue homogenizer Precellys 24. Particulate was removed by 30 min centrifugation at 13,000*g*.

Western blot analyses were performed according to standard protocols using the following primary antibodies: anti-pSer473AKT and anti-AKT (Cell Signaling), anti-insulin receptor β-chain (Cell Signaling), anti-pTyr1162/1163 insulin receptor (Santa Cruz Biotechnology), and anti-IRS1 and anti-pSer307 IRS1 (Cell Signaling). Equal protein loading was assured by Ponceau S staining. Signals were quantified using ImageQuant software. Signal intensities obtained with phosphospecific antibodies were normalized for those obtained with antibodies against total proteins.

Immunoprecipitation and chemical cross-linking of insulin receptor. HEK293T cells were cotransfected with pCDNA-IR-Rluc, pCDNA-Neu1-YFP, and pCMV-CathA plasmids. After 48 h, the cells were treated or not with 20 mmol/L insulin for 15 min, washed with ice-cold PBS, collected and resuspended in RIPA buffer containing 0.2 mmol/L dithiobis(succinimidyl propionate), vortexed, placed on ice for 30 min, cleared by centrifugation (20 min at 12,000*g* and 4°C), and incubated with anti-insulin receptor β-chain antibodies (Cell Signaling) for 4 h at 4°C. Antibody complexes were precipitated by overnight incubation with protein A–agarose (Santa Cruz Biotechnology). Proteins were eluted by boiling the resin in Laemmli sample buffer containing 50 mmol/L dithiothreitol and analyzed by Western blotting using anti-insulin receptor β-chain (Cell Signaling) and anti-Neu1 antibodies (49).

Confocal immunofluorescence microscopy. Forty-eight hours after transfection with pCDNA3-IRK-Rluc, pCDNA-Neu1-YFP, and pCMV-CathA plasmids, HEK293T cells were washed with ice-cold PBS, fixed in 4% paraformaldehyde and 4% sucrose in PBS for 5 min, and rinsed three times with PBS. Cells were permeabilized by 0.25% Triton X-100 for 10 min, blocked for 1 h in 3% horse serum and 0.1% Triton X-100, and costained with mouse anti-insulin receptor β-chain (Cell Signaling) (1:400) and rabbit anti-Neu1 (1:100) antibodies in 3% horse serum–PBS. Cells were counterstained with Oregon Green 488–conjugated anti-rabbit IgG antibodies and Texas Red–conjugated goat anti-mouse antibodies (1:1,000; Molecular Probes). Slides were studied on a Zeiss LSM510 inverted confocal microscope. Images were processed using the LSM image browser software (Zeiss) and Photoshop (Adobe) to increase contrast.

***D*: Unchanged Ser phosphorylation of IRS-1. Total liver homogenates obtained as described above were analyzed by Western blotting using antibodies against total IRS-1 or IRS-1 phosphorylated at Ser307 residue. *E*: Insulin-dependent phosphorylation of AKT in cultured skin fibroblasts from normal individual (Control) and from a sialidosis patient with complete deficiency of Neu1 (Sialidosis). Cells were serum starved overnight, treated or not for 90 min with purified mouse Neu1 (0.5 mU of enzymatic activity per 1 mL of medium), and then treated for 15 min with 20 nmol/L insulin. Protein (20 μg) from cell lysates was analyzed by Western blotting with monoclonal antibodies against pSer473-AKT or against total AKT. Bar graph shows average data from three independent experiments, and the panel is the representative data from one experiment.**

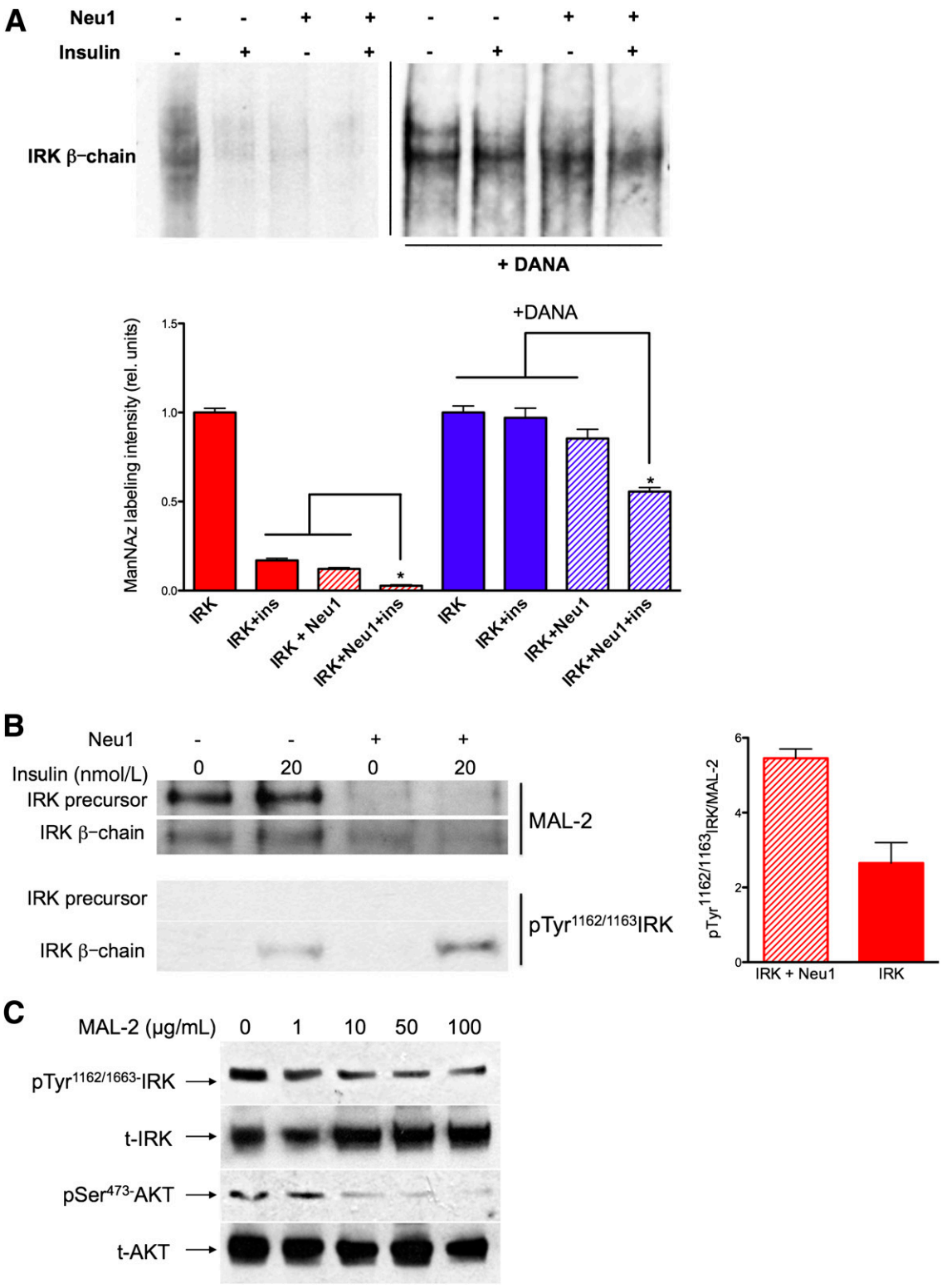

FIG. 3. Insulin-dependent desialylation of IRK by Neu1. *A*: ManNAz labeling of sialic acid in the glycan chains of the β-subunit of IRK expressed in HEK cells alone or coexpressed with Neu1 and CathA and pretreated or not with 1 mmol/L DANA for 1 h. After 10 min of incubation with 20 nmol/L insulin, cells were solubilized with 1% octylglucoside and treated with biotin phosphane, and IRK was purified using affinity chromatography and analyzed by blotting with streptavidin-HRP. Bar graph shows quantification (mean values and SD) of signal intensities using ImageQuant software. In each experiment, the values were normalized to the intensities of IRK staining without Neu1 and insulin. The combined effect of Neu1 overexpression and insulin on ManNAz labeling was significantly (*$P < 0.05$) higher than that of each condition separately. *B*: IRK samples obtained as described above were studied by MAL-2 lectin blot (*top*) or Western blotting with anti-pTyr1162/1163 IRK antibodies. Equal loading of the IRK was verified with antibodies against IRK (not shown). Bar graph shows quantification (mean values and SD) of signal intensities for the β-subunit of IRK using ImageQuant software. *C*: MAL-2 blocks insulin-induced activation of IRK and AKT in a dose-dependent manner. HEK cells coexpressing CBP-tagged IRK and Neu1/CathA were treated with unlabeled MAL-2 lectin in a concentration of 0, 1, 10, 50, and 100 μg/mL of cell medium 30 min before induction with 20 nmol/L insulin for 10 min. Cells were solubilized in 50 mmol/L HEPES, pH 7.4, containing 0.1 mmol/L EDTA, 150 mmol/L sodium chloride, 2 mmol/L phenylmethylsulfonyl fluoride, 1% NP40, 2.5% sodium deoxycholate, and full protease and phosphatase inhibitor cocktail and subjected to immunoprecipitation using anti-IRK antibodies and Western blotting. Blots were stained with anti-pSer473 AKT and anti-AKT, anti-IRK β-chain, and anti-pTyr1162/1163 IRK antibodies as indicated.

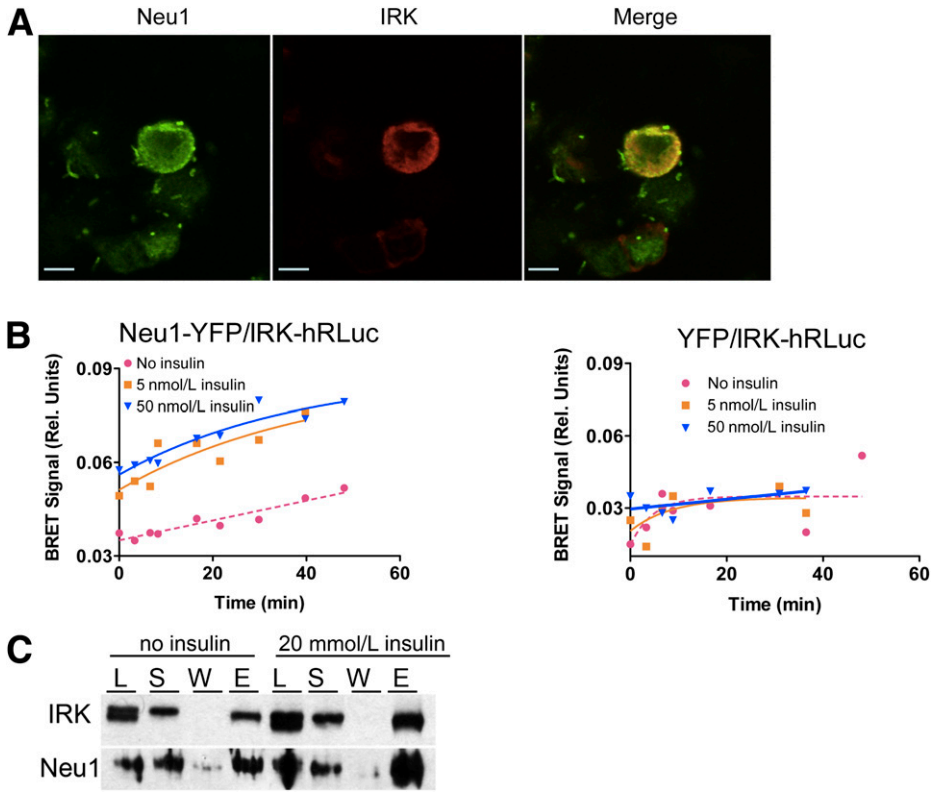

FIG. 4. Insulin-induced interaction between IRK and Neu1 on the cell surface. *A*: Colocalization of IRK and Neu1 on the plasma membrane. HEK cells expressing Neu1-YFP and IRK-hRluc chimeric proteins were fixed with paraformaldehyde, permeabilized by Triton X-100, and costained with mouse anti-insulin receptor β-chain (Cell Signaling) (1:400) and rabbit anti-Neu1 (1:100) antibodies. Cells were then counterstained with Oregon Green 488–conjugated anti-rabbit IgG antibodies and Texas Red–conjugated goat anti-mouse antibodies (1:1,000; Molecular Probes). Slides were studied on a Zeiss LSM510 inverted confocal microscope. *B*: Detection of interaction between IRK and Neu1 by BRET. HEK cells expressing Neu1-YFP and IRK-hRluc (*left*) or YFP and IRK-hRluc (*right*) were treated with coelenterazine H in the absence or in the presence of 5 and 50 nmol/L insulin, and the BRET signal was calculated as the ratio of light intensity emitted by IRK-hRluc (530 nm) and Neu1-YFP (480 nm). In the absence of insulin, only the background levels of energy transfer between Neu1-YFP and IRK-hRluc are observed, whereas incubation of cells with insulin at physiological concentration of 5 nmol/L results in the appearance of BRET signal. *C*: Coimmunoprecipitation of IRK and Neu1. Hek293T cells overexpressing IRK-hRluc, Neu1-YFP, and CathA plasmids were treated or not with 20 nmol/L insulin for 15 min, washed with ice-cold PBS, and lysed in RIPA buffer containing dithiobis(succinimidyl propionate) cross-linker. After removal of cell debris by centrifugation, supernatants were subjected to immunoprecipitation using anti-insulin receptor β-chain antibodies. Proteins in cell lysate (L), supernatant of cell extract (S), protein A agarose washes (W), and eluate (E) were analyzed by Western blotting using anti-insulin receptor β-chain and anti-Neu1 antibodies.

Analysis of interaction between Neu1 and IRK by BRET. BRET analysis was performed as previously described (28) in HEK293T cells transfected with pCDNA3-IRK-Rluc, pCDNA-Neu1-YFP, and pCMV-CathA in the presence of 0–100 nmol/L insulin. The BRET signal was calculated as the ratio of light intensity emitted by IRK-Rluc (530 nm) and Neu1-YFP (480 nm). The values were corrected by the background signal measured in cells expressing only IRK-Rluc.

Purification and MS analysis of recombinant IRK. HEK293T cells were transfected with pCDNA1.3-IRK-Taptag plasmid encoding human IRK with COOH-terminal TAP tag (Invitrogen), pCMV-Neu1, and pCMV-CathA (49). Forty-eight hours after transfection, the cells were treated or not with 20 nmol/L insulin for 10 min, washed with ice-cold PBS, harvested, lysed by sonication in a buffer containing 40 mmol/L Tris, 300 mmol/L KCl, 2 mmol/L dithiothreitol, 2 mmol/L EDTA, 2 mmol/L phenylmethylsulfonyl fluoride, pH 7.4, and protease and phosphatase inhibitors (Roche), and centrifuged at 100,000*g* for 1 h at 4°C. Pellets were resuspended in the lysis buffer depleted of EDTA and containing 2 mmol/L $CaCl_2$, 0.1% NP-40, and 1% octylglucoside. The homogenates were sonicated for 5 s and gently stirred at 4°C overnight to solubilize proteins. The suspension was then centrifuged at 13,000*g* for 30 min. Affinity purification of TAP-tagged IRK was performed using calmodulin resin (Stratagene) according to the manufacturer's protocol. After separation by SDS-PAGE, the gel pieces containing the IRK were excised and digested with trypsin (Promega). The tryptic peptides were analyzed by nano liquid chromatography mass spectrometry using an Eksigent nano-LC LTQ-Orbitrap mass spectrometer system (Thermo Fisher Scientific) as previously described (50). Assignments of phosphorylation sites were validated through manual inspection of relevant tandem MS (MS/MS) spectra.

Analysis of IRK sialylation by metabolic labeling with 2-azidoacetylmannosamine. HEK293T cells transfected with pCDNA1.3-IRK-Taptag or cotransfected with pCDNA1.3-IRK-Taptag, pCMV-Neu1, and pCMV-CathA were cultured for 48 h in the medium containing 70 μmol/L peracetylated *N*-azidoacetylmannosamine (ManNAz). Cell extract was passed through avidin-agarose (Sigma-Aldrich) to remove endogenously biotinylated proteins and incubated for 3 h at 37°C with 50 μmol/L biotin-phosphane (Fisher). IRK purified as above was resolved by SDS-PAGE and transferred to nitrocellulose membranes. Blots were stained with horseradish peroxidase (HRP)–conjugated streptavidin (1:1,000) and an enhanced chemiluminescence kit.

Lectin blot. Affinity-purified IRK samples were resolved by SDS-PAGE and transferred to nitrocellulose membranes. Blots were stained with biotinylated MALII (Vector Laboratories), followed by HRP-conjugated streptavidin and an enhanced chemiluminescence kit. Autophosphorylation of IRK was measured with anti-pTyr1162/1163 antibodies and the total amount of receptor with anti–calmodulin-binding peptide (anti-CBP) polyclonal antibodies (Abgene).

ACKNOWLEDGMENTS

This work was partially supported by research grants from the Canadian Diabetes Association and the Canadian Institutes for Health Research to A.V.P.

No potential conflicts of interest relevant to this article were reported.

L.D., V.S., A.F., X.P., and É.B. conducted experiments and analyzed the data. P.T., G.A.M., N.H., A.H., and A.V.P. designed experiments and analyzed the data. A.M. and T.I. provided

essential materials for the study and analyzed the data. C.W.C. designed experiments, analyzed the data, and provided essential materials for the study. All authors participated in writing the manuscript and approved it as submitted. A.V.P. is the guarantor of this work and, as such, had full access to all the data in the study and takes responsibility for the integrity of the data and the accuracy of the data analysis.

The authors thank Shu Pei Wang (Sainte-Justine University Hospital Research Center) for technical advice.

REFERENCES

1. DeFronzo RA, Ferrannini E. Insulin resistance. A multifaceted syndrome responsible for NIDDM, obesity, hypertension, dyslipidemia, and atherosclerotic cardiovascular disease. Diabetes Care 1991;14:173–194
2. Kahn SE. The importance of the beta-cell in the pathogenesis of type 2 diabetes mellitus. Am J Med 2000;108(Suppl. 6a):2S–8S
3. Martin BC, Warram JH, Krolewski AS, Bergman RN, Soeldner JS, Kahn CR. Role of glucose and insulin resistance in development of type 2 diabetes mellitus: results of a 25-year follow-up study. Lancet 1992;340:925–929
4. Taniguchi CM, Emanuelli B, Kahn CR. Critical nodes in signalling pathways: insights into insulin action. Nat Rev Mol Cell Biol 2006;7:85–96
5. Jiang ZY, Zhou QL, Holik J, et al. Identification of WNK1 as a substrate of Akt/protein kinase B and a negative regulator of insulin-stimulated mitogenesis in 3T3-L1 cells. J Biol Chem 2005;280:21622–21628
6. Knutson VP. Cellular trafficking and processing of the insulin receptor. FASEB J 1991;5:2130–2138
7. Dresner A, Laurent D, Marcucci M, et al. Effects of free fatty acids on glucose transport and IRS-1-associated phosphatidylinositol 3-kinase activity. J Clin Invest 1999;103:253–259
8. Griffin ME, Marcucci MJ, Cline GW, et al. Free fatty acid-induced insulin resistance is associated with activation of protein kinase C theta and alterations in the insulin signaling cascade. Diabetes 1999;48:1270–1274
9. Tanti JF, Grémeaux T, van Obberghen E, Le Marchand-Brustel Y. Serine/threonine phosphorylation of insulin receptor substrate 1 modulates insulin receptor signaling. J Biol Chem 1994;269:6051–6057
10. Yu C, Chen Y, Cline GW, et al. Mechanism by which fatty acids inhibit insulin activation of insulin receptor substrate-1 (IRS-1)-associated phosphatidylinositol 3-kinase activity in muscle. J Biol Chem 2002;277:50230–50236
11. Hori SS, Kurland IJ, DiStefano JJ 3rd. Role of endosomal trafficking dynamics on the regulation of hepatic insulin receptor activity: models for Fao cells. Ann Biomed Eng 2006;34:879–892
12. Sesti G, Federici M, Lauro D, Sbraccia P, Lauro R. Molecular mechanism of insulin resistance in type 2 diabetes mellitus: role of the insulin receptor variant forms. Diabetes Metab Res Rev 2001;17:363–373
13. Hwang JB, Hernandez J, Leduc R, Frost SC. Alternative glycosylation of the insulin receptor prevents oligomerization and acquisition of insulin-dependent tyrosine kinase activity. Biochim Biophys Acta 2000;1499:74–84
14. Elleman TC, Frenkel MJ, Hoyne PA, et al. Mutational analysis of the N-linked glycosylation sites of the human insulin receptor. Biochem J 2000; 347:771–779
15. Sparrow LG, Lawrence MC, Gorman JJ, et al. N-linked glycans of the human insulin receptor and their distribution over the crystal structure. Proteins 2008;71:426–439
16. Leconte I, Auzan C, Debant A, Rossi B, Clauser E. N-linked oligosaccharide chains of the insulin receptor beta subunit are essential for transmembrane signaling. J Biol Chem 1992;267:17415–17423
17. Pshezhetsky AV, Hinek A. Where catabolism meets signalling: neuraminidase 1 as a modulator of cell receptors. Glycoconj J 2011;28:441–452
18. Seyrantepe V, Hinek A, Peng J, et al. Enzymatic activity of lysosomal carboxypeptidase (cathepsin) A is required for proper elastic fiber formation and inactivation of endothelin-1. Circulation 2008;117:1973–1981
19. Seyrantepe V, Iannello A, Liang F, et al. Regulation of phagocytosis in macrophages by neuraminidase 1. J Biol Chem 2010;285:206–215
20. Vinogradova MV, Michaud L, Mezentsev AV, et al. Molecular mechanism of lysosomal sialidase deficiency in galactosialidosis involves its rapid degradation. Biochem J 1998;330:641–650
21. Bouvier M, Heveker N, Jockers R, Marullo S, Milligan G. BRET analysis of GPCR oligomerization: newer does not mean better. Nat Methods 2007;4: 3–4; author reply 4
22. Trost M, English L, Lemieux S, Courcelles M, Desjardins M, Thibault P. The phagosomal proteome in interferon-gamma-activated macrophages. Immunity 2009;30:143–154
23. Arabkhari M, Bunda S, Wang Y, Wang A, Pshezhetsky AV, Hinek A. Desialylation of insulin receptors and IGF-1 receptors by neuraminidase-1 controls the net proliferative response of L6 myoblasts to insulin. Glycobiology 2010;20:603–616
24. Surwit RS, Kuhn CM, Cochrane C, McCubbin JA, Feinglos MN. Diet-induced type II diabetes in C57BL/6J mice. Diabetes 1988;37:1163–1167
25. Ellis L, Clauser E, Morgan DO, Edery M, Roth RA, Rutter WJ. Replacement of insulin receptor tyrosine residues 1162 and 1163 compromises insulin-stimulated kinase activity and uptake of 2-deoxyglucose. Cell 1986;45:721–732
26. Lukong KE, Elsliger MA, Chang Y, et al. Characterization of the sialidase molecular defects in sialidosis patients suggests the structural organization of the lysosomal multienzyme complex. Hum Mol Genet 2000;9:1075–1085
27. Durand S, Feldhammer M, Bonneil E, Thibault P, Pshezhetsky AV. Analysis of the biogenesis of heparan sulfate acetyl-CoA:alpha-glucosaminide N-acetyltransferase provides insights into the mechanism underlying its complete deficiency in mucopolysaccharidosis IIIC. J Biol Chem 2010;285: 31233–31242
28. Rikova K, Guo A, Zeng Q, et al. Global survey of phosphotyrosine signaling identifies oncogenic kinases in lung cancer. Cell 2007;131:1190–1203
29. Tavaré JM, Denton RM. Studies on the autophosphorylation of the insulin receptor from human placenta. Analysis of the sites phosphorylated by two-dimensional peptide mapping. Biochem J 1988;252:607–615
30. Laughlin ST, Agard NJ, Baskin JM, et al. Metabolic labeling of glycans with azido sugars for visualization and glycoproteomics. Methods Enzymol 2006;415:230–250
31. Percherancier Y, Berchiche YA, Slight I, et al. Bioluminescence resonance energy transfer reveals ligand-induced conformational changes in CXCR4 homo- and heterodimers. J Biol Chem 2005;280:9895–9903
32. Issad T, Boute N, Pernet K. A homogenous assay to monitor the activity of the insulin receptor using bioluminescence resonance energy transfer. Biochem Pharmacol 2002;64:813–817
33. Versteyhe S, Blanquart C, Hampe C, et al. Insulin receptor substrates-5 and -6 are poor substrates for the insulin receptor. Mol Med Rep 2010;3:189–193
34. Lorenz WW, McCann RO, Longiaru M, Cormier MJ. Isolation and expression of a cDNA encoding *Renilla reniformis* luciferase. Proc Natl Acad Sci USA 1991;88:4438–4442
35. Gammeltoft S. Insulin receptors: binding kinetics and structure-function relationship of insulin. Physiol Rev 1984;64:1321–1378
36. Miyagi T. Aberrant expression of sialidase and cancer progression. Proc Jpn Acad, Ser B, Phys Biol Sci 2008;84:407–418
37. Yamaguchi K, Hata K, Koseki K, et al. Evidence for mitochondrial localization of a novel human sialidase (NEU4). Biochem J 2005;390:85–93
38. Monti E, Preti A, Venerando B, Borsani G. Recent development in mammalian sialidase molecular biology. Neurochem Res 2002;27:649–663
39. Pshezhetsky AV, Ashmarina M. Lysosomal multienzyme complex: biochemistry, genetics, and molecular pathophysiology. Prog Nucleic Acid Res Mol Biol 2001;69:81–114
40. d'Azzo A, Andria G, Strisciuglio G, Galjaard H. Galactosialidosis. In *The Metabolic and Molecular Bases of Inherited Disease*, 8th ed. Scriver CRBA, Sly WS, Valle D., Eds. New York, McGraw-Hill, 2001, p. 3811–3826
41. Thomas GH. Disorders of glycoprotein degradation: α-mannosidosis, β-mannosidosis, fucosidosis, and sialidosis. In *The Metabolic and Molecular Bases of Inherited Disease*. Scriver CRBA, Sly WS, Valle D, Eds. New York, McGraw-Hill, 2001
42. Hinek A, Pshezhetsky AV, von Itzstein M, Starcher B. Lysosomal sialidase (neuraminidase-1) is targeted to the cell surface in a multiprotein complex that facilitates elastic fiber assembly. J Biol Chem 2006;281:3698–3710
43. Miyagi T, Yamaguchi K. Mammalian sialidases: physiological and pathological roles in cellular functions. Glycobiology 2012;22:880–896
44. Hinek A, Bodnaruk TD, Bunda S, Wang Y, Liu K. Neuraminidase-1, a subunit of the cell surface elastin receptor, desialylates and functionally inactivates adjacent receptors interacting with the mitogenic growth factors PDGF-BB and IGF-2. Am J Pathol 2008;173:1042–1056
45. Sun JV, Tepperman HM, Tepperman J. Lipid composition of liver plasma membranes isolated from rats fed a high glucose or a high fat diet. J Nutr 1979;109:193–201
46. van Amelsvoort JM, van der Beek A, Stam JJ. Effects of the type of dietary fatty acid on the insulin receptor function in rat epididymal fat cells. Ann Nutr Metab 1986;30:273–280
47. Rusciani A, Duca L, Sartelet H, et al. Elastin peptides signaling relies on neuraminidase-1-dependent lactosylceramide generation. PLoS ONE 2010; 5:e14010
48. Sladek R, Rocheleau G, Rung J, et al. A genome-wide association study identifies novel risk loci for type 2 diabetes. Nature 2007;445:881–885
49. Manolio TA, Collins FS, Cox NJ, et al. Finding the missing heritability of complex diseases. Nature 2009;461:747–753
50. Sardiello M, Palmieri M, di Ronza A, et al. A gene network regulating lysosomal biogenesis and function. Science 2009;325:473–477